PHYSICAL REVIEW A VOLUME 1, NUMBER 1 JANUARY 1970

Decay of the Velocity Autocorrelation Function*

B. J. Alder and T. E. Wainwright
Lawrence Radiation Laboratory, University of California, Livermore, California 94550
(Received 10 July 1969)

Molecular-dynamic studies of the behavior of the diffusion coefficient after a long time s have shown that the velocity autocorrelation function decays as s^{-1} for hard disks and as $s^{-3/2}$ for hard spheres, at least at intermediate fluid densities. A hydrodynamic similarity solution of the decay in velocity of an initially moving volume element in an otherwise stationary compressible viscous fluid agrees with a decay of $(\eta s)^{-d/2}$, where η is the viscosity and d is the dimensionality of the system. The slow decay, which would lead to a divergent diffusion coefficient in two dimensions, is caused by a vortex flow pattern which has been quantitatively compared for the hydrodynamic and molecular-dynamic calculations.

A previous study[1] of the diffusion coefficient has shown that the velocity autocorrelation function has a long positive tail, indicating a surprising persistence of velocities. Subsequently,[2] the collective nature of this persistence was established by the observation that the value of the diffusion coefficient depends strongly on the number of particles, particularly in two dimensions where the results did not seem to converge as larger systems were investigated. Finally, by studying the velocity correlation between a molecule and its neighborhood, a vortex flow pattern was found on a microscopic scale which could qualitatively explain the tail. Since the persistence of the vortex flow is long compared to the mean collision time, it is natural to ask whether a hydrodynamic model could calculate such vortex motion, and hence, the behavior of the velocity autocorrelation function for long times. This paper addresses itself to that question.

In such a hydrodynamic model, a fluid is imagined to be at rest except that a small volume element is given an initial velocity. A compression wave develops in front of this region and a rarefaction wave to the rear. When the sound waves have separated, the residual flow is in the form of a double vortex in two dimensions, or a vortex ring in three dimensions. At late times, the circulatory flow approaches that of an incompressible fluid, and hence the velocity decays solely due to the influence of the shear viscosity. It should be emphasized at the outset that this hydrodynamic model differs conceptually from the Stokes-Einstein model which also relates the diffusion coefficient to the viscosity. In that model, a sphere representing a molecule is assumed to slow down adiabatically in a viscous fluid; that is, the retarding force at each instant of time is assumed to be the steady-state value, which is proportional to the velocity, so that the velocity decays exponentially. In the model described here, on the other hand, a transient solution of the Navier-Stokes equation is carried out to find the long-time behavior of the initially moving volume element.

The initially moving volume element is made equal in size to the average volume per molecule and is given a velocity comparable to the root-mean-square molecular velocity. The subsequent motion of the fluid is then calculated by direct numerical integration of the Navier-Stokes equation.[3] Both Eulerian and Lagrangian formulations have been used successfully. A comparison of the flow pattern between the hydrodynamic and molecular-dynamic calculation at a fairly late time is given in Fig. 1. The nearly quantitative agreement obtained lends credence to the applicability of the model. The values for the viscosity η and $y = Pv/NkT - 1$ used in the hydrodynamic calculation were obtained from molecular-dynamic calculations at the same density. The comparison in Fig. 1 was made at a fairly late time, so that the flow pattern had approached the hydrodynamic regime, but not so late that there was any interference from the sound waves coming over the periodic border of the finite system, nor so late that the velocity had decayed to such a small value as to prevent an accurate determination. A correction of $1/N - 1$ has been added to the velocity autocorrelation function as calculated by molecular dynamics. This is because whenever a given molecule has a velocity v, the average velocity of the other molecules is $-v/N - 1$ in a system of N molecules where momentum is conserved.

Figure 2 illustrates, in the case of hard spheres, the agreement of the autocorrelation function $\rho(s)$ from the molecular-dynamic calculation with that from the hydrodynamic calculation. The latter is simply the velocity at the center of the flow pattern divided by the initial velocity. The two disagree at short times, as might be expected. The molecular-dynamic velocity autocorrelation function shows an initial exponential decay lasting for a few mean collision times s. However, at times great-

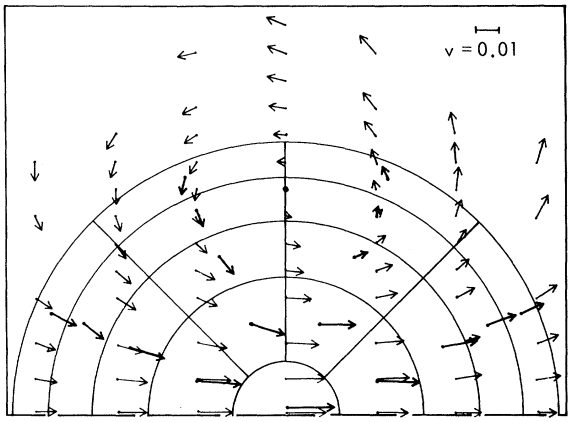

FIG. 1. Statistically averaged velocity field around a central disk from molecular dynamics (heavy arrows) compared to that given by the hydrodynamic model (light arrows). Because of symmetry only half the plane is shown. The scale of distance is indicated by the size of the central disk as shown by the smallest half-circle. The sizes of the other four concentric circles have been determined so as to include roughly six neighboring particles each. These semicircles have been partitioned further into four parts, as indicated by the lines, so as to have a measure of direction relative to the velocity vector of the central particle at zero time. The size of the arrows indicates the magnitude of the velocity (the scale of velocity is indicated as 0.01 of the initial velocity in the upper right-hand corner) and the direction of the arrow is determined by the parallel and perpendicular components of the velocity (relative to that of the central particle initially) averaged over all the particles in that section at a particular time. The arrow is hence drawn at the center of the section. A correction of $1/N-1$ has been added to the parallel component. The comparison is made at 9.9 collision times where the molecular-dynamic and hydrodynamic velocity autocorrelations begin to nearly agree, as seen on the graph by the velocity vectors of the central particle. (See also Fig. 3.) In the molecular-dynamics run, 224 hard disks were used at an area relative to close packing of 2. For the hydrodynamic run, the conditions are given in Table I.

er than about 10 mean collision times, both calculations show a decay like $s^{-3/2}$.

Figure 3 illustrates the same agreement at various densities in the case of hard disks where the decay is like s^{-1}. Figure 3 shows furthermore that the $1/N-1$ correction brings into agreement the velocity autocorrelation functions calculated in molecular-dynamic systems of various sizes and that the long-time behavior of the hydrodynamic solution is independent of the initial velocity. It was also found that the long-time hydrodynamic solution does not depend upon the bulk viscosity. Heat conductivity was not included in the hydrodynamic calculation. The late-time kinks seen in Fig. 3 in the velocity autocorrelation functions calculated for 504 particle systems are caused by the arrival of sound waves from the periodic images. The arrival time of these interferences can be predicted by the hydrodynamical model.

A simple analysis of the hydrodynamical model

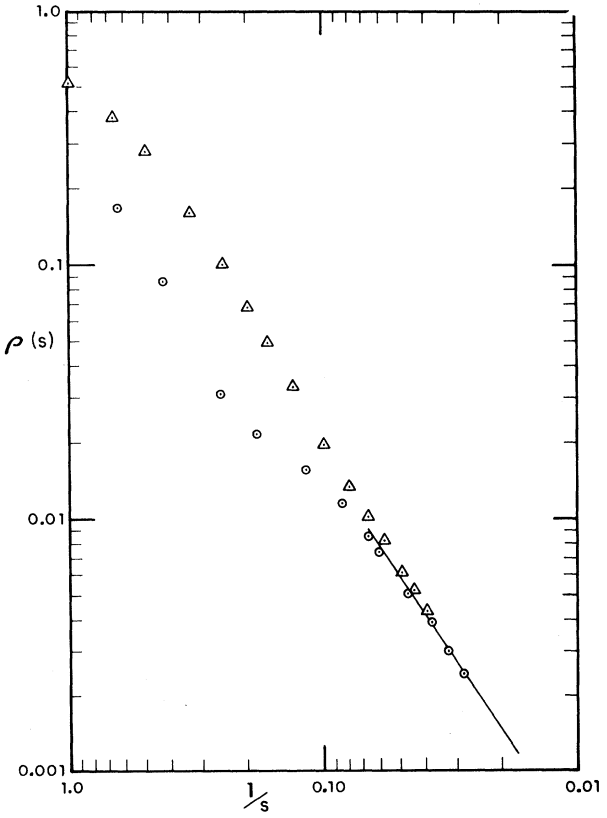

FIG. 2. Comparison of the velocity autocorrelation function $\rho(s)$ as a function of time (in terms of mean collision times s) between the hydrodynamic model (circles) and a 500-hard-sphere molecular-dynamic calculation (triangles) at a volume relative to close packing of 3 on a log-log plot. The straight line is drawn with a slope corresponding to $s^{-3/2}$. To the molecular dynamics $\rho(s)$ a correction of $1/N-1$ has been added. Furthermore, the function has only been graphed up to the time where serious interference between neighboring periodically repeated systems is indicated. In the hydrodynamic calculation the viscosity predicted by the Enskog theory has been used while the molecular-dynamic calculations indicate a 2% larger value. A value of pv/NkT of 3.03 was employed, and the initial velocity of the fluid volume element was normalized to unity for comparison purposes. If the initially moving cylindrical region is made to have the same volume as that corresponding to the volume per particle in the molecular system, a distance and hence a time scale can be obtained to make the above comparison.

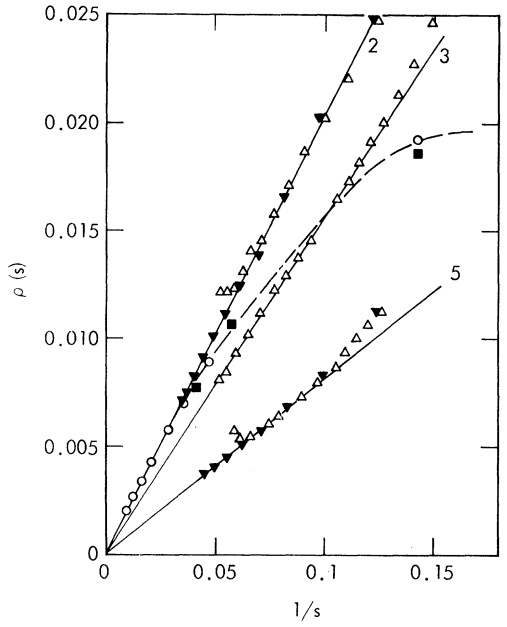

FIG. 3. The decay of the velocity autocorrelation function at large times for hard disks at three densities: $A/A_0 = 2, 3$, and 5. The closed and open triangles refer to molecular-dynamic runs of 986 and 504 particles, respectively. A $1/N-1$ correction to the molecular-dynamic results has been applied. At A/A_0 of 2 and 5 the 504-particle results include the initial deviations due to the interference of neighboring cells at the boundary while all other results have not been plotted beyond the point where serious interference is indicated. The dashed line represents the results of a hydrodynamic run at A/A_0 of 2 (see Table I for conditions) in which the initially moving square area element was given two different velocities, the root-mean-square molecular velocity (squares) and that $\frac{1}{14}$th as large (circles).

shows that a similarity solution exists for the circulatory flow at late times. The linear dimensions of the flow pattern increase at $(\nu s)^{1/2}$ and, since total momentum is conserved, the velocity decays as $(\nu s)^{-d/2}$, where ν is the kinematic viscosity (η divided by the density) and d is the dimensionality of the system. This result verifies the observed behavior.

Table I lists the values of the decay constants α, found by molecular dynamics in two dimensions, where $\rho(s) = \alpha s^{-1}$. Since the hydrodynamic model predicts $\rho(s)$ is proportional to $(\nu s)^{-1}$, $\alpha_H = \alpha\eta s/\eta_0 s_0 = \alpha\eta/\eta_0 y$ should be a constant; the collision rate being proportional to y. The zero subscript indicates the low-density Boltzmann values for the reference system. The value of α_H is π^{-1}, as accurately as it can be determined from the numerical hydrodynamic calculations at a number of different densities and also according to the analytic asymptotic solution. This solution does, however, depend on the empirically supported assumption that the two sound waves carry off $\frac{1}{2}$ of the original momentum, independent of all parameters involved in the calculation, the remaining half being involved in the vortex flow.

The slight remaining density dependence of α_H and its small disagreement with the hydrodynamic solution can be ascribed to the unrealistic nature of the hydrodynamical model. The hydrodynamic flow will not carry the molecule appreciably away from the center of the vortex pattern; but, in fact, in an actual system a molecule has a density-dependent probability of diffusing away from the center. At low densities, particularly, intermolecular diffusion can carry molecules away from the center to a distance comparable with the size of the vortex pattern. To account approximately for the diffusive motion, the vortex flow pattern has to be sampled over a spreading Gaussian distribution representing the probability that the molecule has moved away from the center. This argument leads to the following correction factor F:

$$F = \frac{\int \exp(-r^2 D_0/D_E s)\exp(-r^2\eta_0/\eta s) r\,dr}{\int \exp(-r^2 D_0/D_E s) r\,dr} = \frac{\eta/\eta_0}{D_E/D_0 + \eta/\eta_0}\,.$$

The Enskog value of the diffusion coefficient D_E is used because it is intended to describe only the diffusion of the molecules among its neighbors and not the collective motion of the neighborhood for which the hydrodynamic model is used.

A comparison of the last two columns of Table I shows that this correction factor F accounts for the density dependence of α_H to within a few percent, that is, within the accuracy of the determina-

TABLE I. Values of the decay coefficient α.

A/A_0	α	y	η/η_0	D_E/D_0	$\alpha_H = \alpha\eta/\eta_0 y$	$\alpha_H\pi$	F
2	0.206	2.42	3.39	0.375	0.29	0.91	0.90
3	0.157	1.08	1.66	0.560	0.24	0.76	0.75
5	0.082	0.50	1.29	0.725	0.21	0.66	0.64

tion of α and η/η_0. The above argument leads to the prediction that in the low-density limit $F = \frac{1}{2}$. Thus, the velocity autocorrelation function in two dimensions decays as s^{-1} at any finite density, leading to a divergent diffusion coefficient at any nonzero density. This result is in contradiction to previous theories on the density expansion of the diffusion coefficient away from the low-density limit. The study of the late-time autocorrelation function at very low densities by molecular dynamics is unfortunately very difficult since the system must be so large that a molecule undergoes many collisions before a sound wave travels across the size of the system.

The hydrodynamic model, as discussed so far, cannot reverse the velocity of the region initially in motion, and thus cannot reproduce the negative part of the velocity autocorrelation found at high densities. This deficiency can be remedied at least qualitatively by the inclusion of visco-elastic forces in the Navier-Stokes equations. These forces can be obtained from the autocorrelations of the elements of the stress tensor as calculated by molecular dynamics. A trial calculation at $A/A_0 = 1.4$ has shown that negative autocorrelation functions can be obtained in this way, but that at very late times, in agreement with molecular dynamics, the function becomes again positive and decays like s^{-1}.

We wish to thank E. D. Giroux and J. A. Viecelli for invaluable help with the hydrodynamic calculations and M. A. Mansigh similarly with the molecular-dynamic calculations.

---

*Work performed under the auspices of the U.S. Atomic Energy Commission.

[1]B. J. Alder and T. E. Wainwright, Phys. Rev. Letters 18, 988 (1967).

[2]B. J. Alder and T. E. Wainwright, J. Phys. Soc. Japan, Suppl. 26, 267 (1968).

[3]M. L. Wilkins, in Methods in Computational Physics (Academic Press Inc., New York, 1964), Vol. 3, p. 211.

PHYSICAL REVIEW A VOLUME 1, NUMBER 1 JANUARY 1970

Production of H Atoms in the 3s State by the Impact of Fast Ground-State H Atoms on N_2†

R. H. Hughes, A. R. Filippelli, and H. M. Petefish*
Department of Physics, University of Arkansas, Fayetteville, Arkansas 72701
(Received 26 August 1969)

Cross sections for the production of hydrogen atoms in the 3s state by the impact of ground-state hydrogen atoms on nitrogen molecules have been measured in the kinetic energy range 10–35 keV. The cross-section curve appears to have a maximum at the lower energies of about 4×10^{-18} cm^2. This value is roughly $2\frac{1}{2}$ times less than the maximum cross section for producing 3s atoms through electron capture by proton impact on nitrogen molecules in the same energy range.

INTRODUCTION

Cross sections have been measured for electron capture into the 3s, 3p, and 3d states by proton impact on N_2 in the energy range 10–35 keV.[1] In this paper, we report the measurement of the cross section for production of 3s hydrogen atoms by the impact of ground-state hydrogen atoms on N_2.

This particular reaction is important in understanding the production of H_α light ($n = 3 \rightarrow 2$ transitions) from fast hydrogen atoms in the aurora. Fast protons which are incident on the upper atmosphere will undergo a series of electron capture and stripping reactions as they pass through the atmosphere. These protons will spend much of their fast-particle history in the form of ground-state hydrogen atoms. Hence, collisional excitation of ground-state hydrogen atoms of atmospheric gases could be an important mechanism for the production of the Balmer light, as well as direct electron capture by protons into excited states.